

A Muon Cooling Experiment with Bunched Beams

J. Norem

HEP Division, Argonne National Laboratory, Argonne IL 60439

(Sept 19, 2000)

I. INTRODUCTION

Muon cooling is both the basic idea and the primary uncertainty in the feasibility of high intensity muon facilities. The novelty of periodic solenoidal focusing systems with accelerating and decelerating elements has generated a number of complex problems and a slow learning curve, however. While there are also questions about the proton driver, target, acceleration and ring design of a neutrino source or collider, the parameters of the cooling system also tend to drive the requirements on these other systems.

Even if cooling was straightforward, there are a large number of issues that must be resolved before a useful cooling line could be constructed. Measurement of muon bunches in the presence of backgrounds has never been done, much less with the high precision required for tuning up the cooling line. The beam must be matched in 6 dimensions with the cooling line and this match must be maintained down the length of the line. Alignment, beam losses and beam cooling must be measured to high precision in a very difficult environment. Thus it is highly desirable to produce a facility where cooling could be demonstrated and the problems of muon cooling for large machines could be studied independently.

Nevertheless, a cooling demonstration is difficult. Dark current electrons and x-rays from the rf cavities required for reacceleration seem to preclude making good single track measurements of complete systems. Large backgrounds from a variety of sources, and the difficulty of precision measurements of beam distributions could complicate measurements of bunched beams. In addition the particle distributions are inherently nonlinear and the behavior of particles at the edges of the distributions is important. Finally, the cooling apparatus itself is expensive, and degree of cooling and the required measurement precision are unclear.

The ultimate goal of the experiment is also relevant. Demonstrating muon cooling, is different from demonstrating a prototype cooling system using muons, and developing a facility which can study all the problems of muon cooling in a neutrino source or muon collider has additional requirements. The relevance of a test assembly is reduced the more the design differs from what will ultimately be constructed, but cost constraints must be respected.

In this environment it seems desirable to carefully optimize the cooling system to minimize costs and to provide the maximum experimental opportunity. This means that different options for decay beamlines as well as in-

strumentation, cooling hardware must be compared on the basis of cost, flexibility and relevance to a real facility.

This note starts to identify the problems in the design of a bunched beam cooling experiment, with the aim of evaluating beam requirements, beamline components, experimental precision measurement scenarios and required instrumentation. At this time cooling simulations are converging on designs for 6D emittance cooling, but a complete design does not yet exist, so the exact cooling apparatus is unclear. Likewise, although some work has been done, the design of a beamline which can produce intense bunches of muons is incomplete (and becoming increasingly complex). Nevertheless, it seems very useful to look at what measurements can be made, how they would be made and what problems might be encountered.

II. COOLING

Studies of muon cooling were done primarily with specialized Monte Carlo programs ICOOL [1] and DPGEANT [2], which are able to track particles through the rf and solenoidal magnetic fields of the cooling line. Recently analytical approaches have become available which can simulate cooling on a more elementary level. This analytical approach makes it possible to do many operations, such as parameter searches, more easily [3] [4]. In the Kim-Wang parameterization, cooling is neatly described by a matrix equation,

$$\frac{d}{ds} \begin{vmatrix} \epsilon \\ L \end{vmatrix} = \begin{pmatrix} \eta & -\eta\kappa\beta \\ -\eta\kappa\beta & \eta \end{pmatrix} \begin{vmatrix} \epsilon \\ L \end{vmatrix} + \begin{vmatrix} \beta\chi \\ 0 \end{vmatrix},$$

where the beam is defined by the emittance, ϵ , and angular momentum, L , and the optical system by $\eta = (dE/ds)/pv$, $\kappa = qB/2p$, and $\chi = (13.6MeV/pv)^2/L_{rad}$, with β , p , v and B referring to the optical beta function, momentum, velocity/ c and B field. The β function obeys the relation

$$\beta''/2 + \kappa^2\beta + 1 + 0.25\beta'^2)/\beta = 0.$$

In this parameterization, the cooling is evaluated by integrating the matrix equation over the length of the cooling line. A number of quite different periodic solenoidal systems have been studied (SFOFO, single flip, Alt Sol, . . .), and cooling is primarily effected by the longitudinal development of the beta function, and the beta functions for many the systems tend to be fairly similar.

Results of cooling calculations are improving from a year ago when the problem of tracking a beam from the

target through a bunching and cooling line was first explored. From a variety of possible lattices, the design has converged on a few candidates which seem to be able to produce some useful cooling, and improvements are being made which produce more cooling at less cost. The SuperFOFO and single flip lattices [5] are described in ref [6] have begun to produce good results, and recent success in improving the SFOFO by Palmer is described in [7] and shown in Figure 1. The apparatus used for this method, shown in Figure 2, is much less demanding than some other designs, but it is still fairly expensive to build. Roughly half the cost is in the rf system and another 30% is in the (fairly low field) superconducting magnets.

While transverse cooling has received considerable attention, longitudinal cooling, done by emittance exchange, has developed more slowly, although recent progress indicates that solenoids with a large bend radius can operate in a single flip geometry to produce 6D emittance cooling.

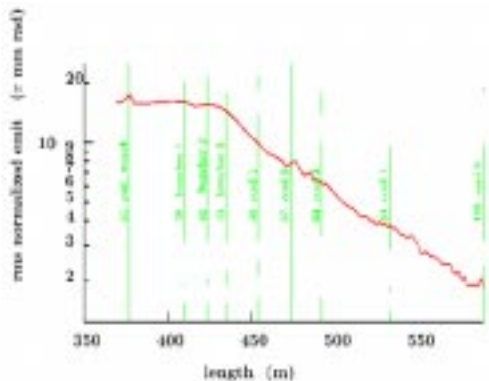


FIG. 1. Recent results with SFOFO cooling.

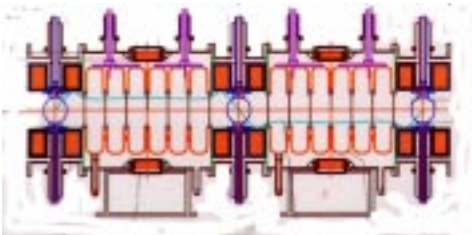


FIG. 2. The SFOFO apparatus.

III. OPTIMIZATION

Since an optimum cooling method has not been selected, it seems desirable to use very general optimization arguments and present normalized plots which can be used to compare different operating modes, rather than detailed numbers or specific solutions.

Using the algebraic expressions for cooling one can make very approximate arguments about the parameter ranges where cooling should be most efficient and

cheapest. The momentum dependence of the cooling process can be studied by setting the solenoidal magnetic field proportional to the momentum and looking at the amount of cooling that is produced in a two meter section. This the basic case is shown in Figure 3. The required rf voltage can be evaluated from the relation $\Delta\epsilon/\epsilon = \Delta p/p = (dE/dx)\Delta x/pv$, with the ionization loss given by the Bethe-Bloch formula [8]

$$-\frac{dE}{dx} = Kz^2 \frac{Z}{A} \frac{1}{\beta^2} \left(0.5 \ln \frac{2m_e c^2 \beta^2 \gamma^2 T_{max}}{I^2} - \beta^2 - \frac{\delta}{2} \right).$$

The scaling or the total magnet cost can be evaluated from the stored energy, $C = U^{0.67}$, where the stored energy, U , is proportional to B^2 .

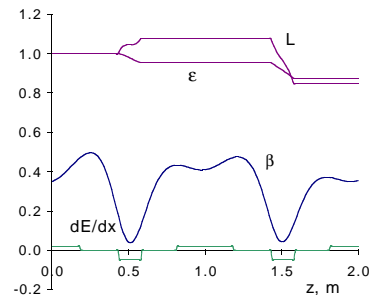


FIG. 3. Cooling with matrices at 120 MeV/c.

The muon momentum is the most obvious variable to consider in designing an experiment. Plotting the emittance reduction, magnet cost, and required rf energy as a function of momentum gives the results shown in Figure 4. The results, normalized to the nominal energy of 180 MeV/c, show that magnet cost drops directly with beam energy. When the emittance reduction is divided by the cost for the rf and magnet systems, again normalizing the results to the nominal beam momentum of 180 MeV/c, one gets the results shown in Figure 5, showing the advantages of cooling with a reduced momentum. Since the rf requirements are directly related to the emittance reduction, better cooling requires more rf voltage and cost reduction must be directed at raising the rf frequency, which lowers the required energy and power of the system.

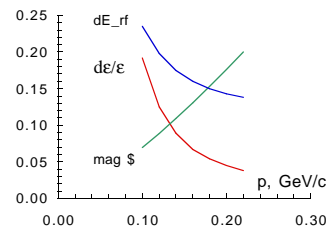


FIG. 4. Momentum Dependence of cooling.

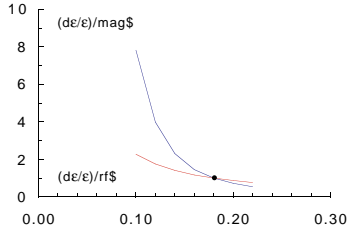


FIG. 5. Cooling efficiency vs. momentum.

There are a number of disadvantages in going to low momentum however, the most obvious is that the longitudinal emittance is increased, at least in the absence of longitudinal cooling. The mechanism for the increase comes because of the shape of the dE/dx curve, which makes the overall emittance grow faster at low β . The expression for this emittance growth has been derived by McDonald [9] and looks like,

$$\frac{d(\Delta E)^2}{dz} \sim \left[\frac{48(\Delta E)^2}{m_e c^2} \frac{(1 - \gamma^2/12)}{\gamma^2 \beta^4 E} + (\gamma^2 + 1) \right],$$

where the first term is proportional to the dE/dx and the second is due to energy straggling fluctuations. The first term, which is larger, is strongly increases with reduced particle velocity and the second term decreases for slower particles. However tracking particles through a section shows that the bunch emittance growth is manageable at lower momenta than simulations are done. This is shown in Figure 6. Longitudinal cooling permits transverse cooling at lower momenta.

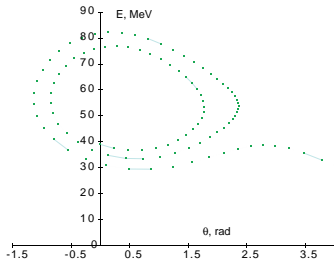


FIG. 6. Emittance growth due to dE/dx .

The rf frequency is the other important variable, since the cost of the cooling hardware is dependent on total energy and power required by the rf. There are two conflicting requirements. The aperture must be large enough to contain the beam but the cost increases with the radius and the longer wavelengths required. The amount of cooling produced in a given section is dependent on the emittance, or the radius of the particle orbit. One can see that small emittances grow toward the equilibrium emittance, defined as

$$\epsilon_{\perp N} = \frac{\beta_{\perp} (14 MeV)^2}{2\beta m c^2 L_R |dE/dx|},$$

and larger emittances damp towards the equilibrium emittance. Injected beam with the equilibrium emittance will not heat or cool. $\Delta\epsilon/\epsilon$ vs $r = \sqrt{\beta\epsilon_{\perp}}$, in cm, is shown in Figure 7.

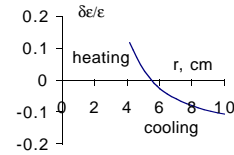


FIG. 7. Cooling vs. radius.

The synchrotron period is a function of the rf frequency, in part because of kinematics, but also because the Kilpatrick limit allows higher gradients to be used at higher frequencies. The dependence is shown in figure 8. The cost of the cooling hardware should scale with the synchrotron period, since a few synchrotron periods are required to let the longitudinal optics develop.

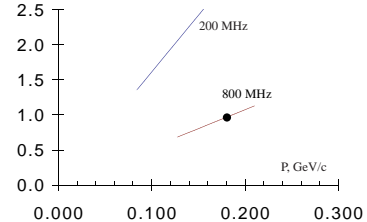


FIG. 8. Synchrotron period vs. momentum and f_{rf} .

The goal of the fastest cooling with the least hardware may be useful. This gives the largest signals with the lowest cost. In general, the primary variables that control the cost and performance of the experiment are the muon momentum and rf frequency. Cooling requires rf, but it requires less at low momenta, and the stored energy is less at high frequencies. Low muon momenta and high rf frequencies seem to give the most efficient cooling, and a detailed optimization is underway.

IV. MEASUREMENTS

The simplest, and perhaps most precise, measurement of cooling can be done by looking at the difference between the beam size with absorbers full and empty, when the rf cavities are used to maintain a constant beam momentum at the end of the line. Note that the (presumably well understood) contributions of the target windows are automatically subtracted off. While emittance measurements are in general not very exact, differential measurements of size and bunch shape should be very precise.

Six dimensional bunch densities can be produced from three dimensional bunch measurements if the bunch distributions can be followed over a significant fraction of a

betatron and synchrotron period. This requires a number of measurements of beam profile in x, y and t, and good information about the development of the beam through the cooling channel. One can expect that beam optics are well understood and the primary uncertainty is likely to be due to the accuracy of the measurements and knowledge of the bunch distributions. Since one is calculating an emittance from a bunch shape, it will be necessary to understand the focusing, as mismatches due to momentum errors can produce significant changes in the beta functions as shown in Figure 9.

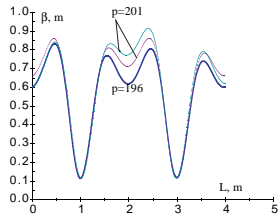


FIG. 9. Changes in β functions when the momentum is changed from 196 to 201 MeV/c.

In order to make consistency checks, is probably desirable to make independent measurements of the six dimensional phase space with an separate spectrometer at the end of the cooling line.

Measurement of correlations will be difficult, but possible, with intense beams.

V. COMPONENTS

A. Beamline

In order to produce a bunched beam muon cooling experiment, one needs a tightly bunched muon beam with small backgrounds. This beam should have a momentum below 200 MeV/c, a large energy spread, $\Delta p/p \sim 0.3$, and a large divergence. The design of the decay line is determined by two effects, first the pions have a decay length, $\lambda[m] = 53.6 p_{\pi} [\text{GeV}/c]$, and the velocity spread of pions and muons with a significant momentum and angular acceptance is large at low energy. This line consists of an initial spectrometer to select a momentum around 400 - 450 MeV/c, (primarily to avoid high energy backgrounds), a decay section with some minimal rf bunching, a second momentum analysis primarily to eliminate the low momentum decay muons, followed by an absorber to reduce the beam energy, as shown in figure 10.

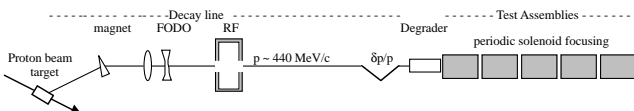


FIG. 10. Beamline components.

The most basic requirement of a beamline is that the pions must be produced from a short proton bunch. It was shown at the Brookhaven AGS that a circulating beam can be bunched into a gaussian width roughly equal to 0.6 % of the bucket length. This method used bunch rotation near transition, where the bunch is naturally short, in addition to excitation of longitudinal quadrupole oscillations to give the shortest possible bunch length, $\sigma = 2$ ns, as shown in Figure 11. This bunching was done with an rf frequency of 3 MHz and a bucket length of 300 ns, so higher rf frequencies should give even shorter bunches. In this experiment, the bunch seemed grossly stable but there was no experimental time for making precision measurements [14].

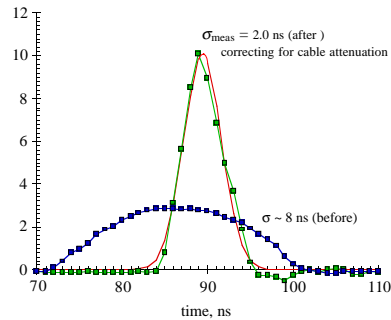


FIG. 11. Bunching at the AGS.

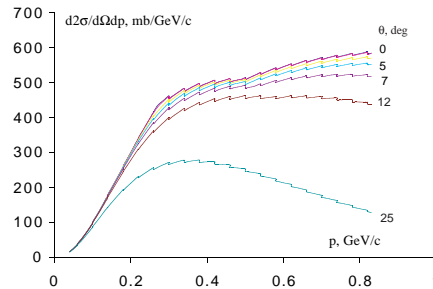


FIG. 12. Positive pion production curves.

The goal of the beam optics is to produce a tight monochromatic muon bunch. Pion / muon beams, produced at a useful momentum, from the target, see Figure 12, can be confined with either quadrupole or solenoidal lines. Quadrupole lines can be either permanent magnet or normal iron magnets. Producing a short bunch at the end presumably requires first a short bunch hitting the target plus a high energy transport line which maintains a tight bunch. The decay line is being simulated using DECAY TURTLE [15]. The particular example uses a 50 m length of 8Q16 quadrupoles packed in a 0.8 m cell giving a $\beta_{max} \sim 2.5$ m, and an emittance of 4000 mm² in x and y, see Figure 13. (The cost of these quads would be about 25 k\$/m, [16] and permanent magnet quads could be built for only slightly more [17]. Solenoidal systems may also be in the same cost range.) Acceleration

is provided by a 100 MeV cell with a frequency of 805 Mhz.

Transporting the beam through a thick degrader at the end of the line primarily accomplishes two things: 1) the degraded beam is produced with an angular divergence due to multiple scattering and energy spread due to straggling roughly matched to the expected cooling line admittance, 2) pions are preferentially absorbed by the material reducing the pion background. The energy and perpendicular momentum distributions produced by ICOOL from an 80 cm long absorber are shown in Figure 14. The absorber is presumed to be in a solenoidal field. The transition between quadrupole and solenoidal focusing can be done in the absorber which *may* simplify the design of this part of the line.

Off energy muons in the beam can be removed by the longitudinal beam optics, but it will take a few meters of the cooling channel, as shown in Figure 15, however this would use valuable cooling hardware. If there is a momentum analysis before the degrader, the ICOOL results show that the energy distribution of particles entering the degrader should be carefully controlled and it should not be necessary to cope with a wide range of off energy muons.

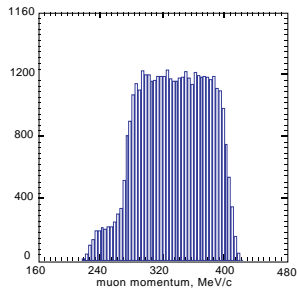


FIG. 13. TURTLE results show muons are confined in 8Q16 quads.

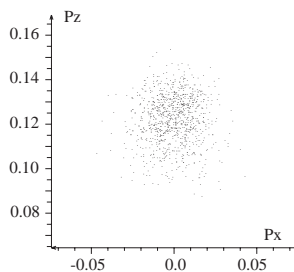


FIG. 14. Momentum exiting the degrader.

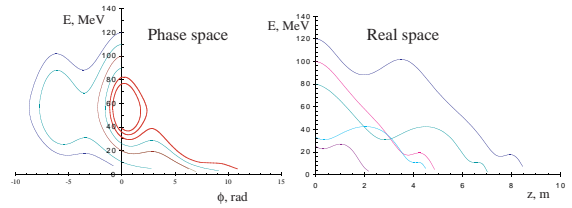


FIG. 15. Self cleaning of bunches.

In general, the angular momentum of the beam is affected by a) the pion production target parameters, b) pion decay, c) the method of transport (solenoid or quadrupole), and d) the environment of the final beam absorber. Since canonical angular momentum is a constant of motion it can be evaluated anywhere, and a particularly useful parameterization is to look at where the trajectory is closest to the magnetic axis [9]. In a solenoidal system the canonical angular momentum is then

$$L_z = r(p_\phi + \frac{\epsilon A_\phi}{c}) = (R_G^2 - R_B^2) \frac{eB}{2c},$$

where R_G , R_B , p_ϕ , and A_ϕ refer to the radius of the guiding ray, the radius of the helical trajectory, the perpendicular momentum component and the circumferential component of the vector potential. In a simple case where quadrupoles are used in the pion production and decay section, the canonical angular momentum is zero until the degrader. The minicooling reduces the radius of helical trajectories, R_B , increasing the angular momentum and the emittance. The process depends on the focusing in the absorber, which must in turn be matched to the decay line on one side and the cooling line on the other. This process is shown in Figure 16 using the Kim-Wang equations, for beta functions that are not matched at either end.

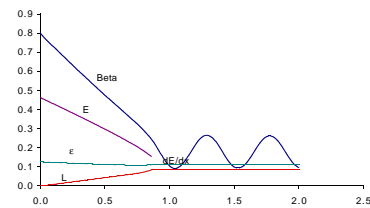


FIG. 16. The beam in the final degrader.

While the final absorber complicates the optics and angular momentum, the effect of putting the Be in the beam has the useful effect of absorbing pions and reducing this contamination in the beam, as shown in Figure 17. This is due to the very large cross sections for large angle pion scattering in the region of the $\Delta(1232)$ resonance. The effect can be roughly approximated by calculating absorption lengths [18] and assuming all interacting particles are removed from the beam, however a more accurate calculation using a hadron cascade Monte

Carlo is probably required. After 100 m of drift about 1% of the pions will remain, and the final absorber will reduce the pion transmission to roughly 0.0005.

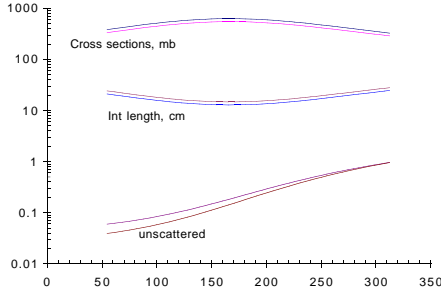


FIG. 17. Pion absorption in the degrader.

B. Backgrounds

There are three primary sources of backgrounds for beam measurements in the neutrino source that must be considered in a bunched beam experiment. The first is the spray of other particles such as kaons, protons and nuclear fragments produced at the target. The second is x rays and dark current electrons produced in the rf cavities, these fluxes have been recently measured in a cavity [19]. The third is due to muons in the beam which are out of time or at the wrong energy to be in the bunch. These are shown schematically in figure 17.

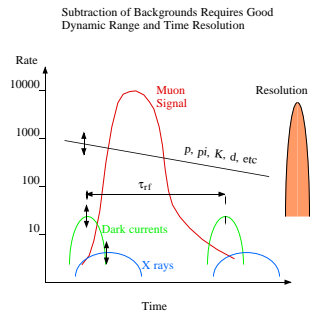


FIG. 18. Good dynamic range and time resolution helps resolve backgrounds.

Backgrounds produced at the target, see Figure 19, must have nearly the same velocity down the decay line to cause serious problems, but the flux of high energy protons, for example, is much larger than pions, and the protons will produce high energy hadronic showers in any material in the beam. Isolation of pions and muons seems to require an initial momentum analysis in the decay beam line. Since protons and kaons are so much heavier than pions, a large $\Delta p/p$ is possible.

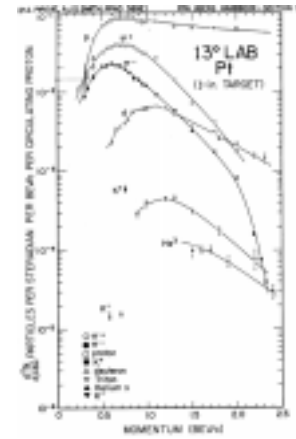


FIG. 19. PPA data on particle production at 3 GeV.

The dark current and x ray problem seems to be caused by the mechanism shown in Figure 20. Operating cavities produce on the order of 1 R/h of x rays at 1 m away, and this corresponds to $\sim 10^7$ 100 kV x rays /cm²/sec, which are radiated somewhat isotropically at low energies. The flux of dark current electrons which produce these x rays is in the range of a few nC/rf pulse, or 10^{10} low energy (but still a few MeV), electrons, which go up and downstream along the axis. This environment is described in a mucool note [19]. The microstructure will be measured in Lab G in November. While coatings [20] and reduction in the rf voltage gradient, (since $\Phi_{e,\gamma} \propto E^{9.6}$ [19]), can both potentially reduce this flux, it seems that the use of single particle detectors in the immediate vicinity of rf cavities is unprecedented.

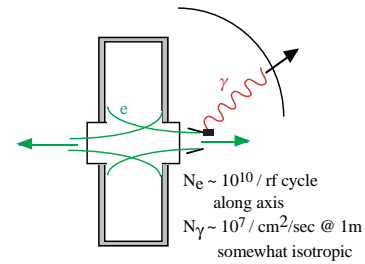


FIG. 20. Dark currents and x rays are produced in cavities.

Since the dark current electrons and muons move at different speeds, ($\Delta\beta \sim 0.15$), the phase of the electrons can be moved relative to the muons by moving the instrumentation along the beam. Since dark current electrons go both directions, their contributions may be pervasive. While the dark current electrons and x rays should be primarily produced over a narrow range of rf phases, it is possible that the dark current electrons could cover a large phase range at any arbitrary point along the line. The transmission of these electrons down the line will depend on their production radius and momentum, and those with rigidities $B\rho < 2B_z R/\pi$, may be trapped in the cusp fields, where R is the electron radius.

Electrons from muon decays will be difficult to separate from the muon bunch and may be an unavoidable background. The contributions can be measured with Cherenkov counters and simulations should give very precise measures of the contribution from this source.

C. Faraday Cups and SEMs

Since the cooling line will have high gradient rf cavities, we expect very high fluxes of dark current electrons and x rays to be associated with them, which are likely to swamp single particle detectors [19]. One can minimize the effects of these backgrounds by maximizing the signal strength and reducing the acceptance for the associated background. Since the electrons and x rays are produced over the length of the whole rf pulse, the resolution time must be as short as possible. With good time resolution, signal to background ratios can possibly improved by factors of

$$F = n_{\mu} \frac{\text{pulselength}}{\text{resolution time}} \sim 10^6 (100\mu\text{s}/100\text{ps}) \sim 10^{12},$$

which would be desirable, and perhaps necessary. Resolutions much less than an rf period could be highly useful because one could time resolve the rf backgrounds. However this severely limits the range of diagnostic techniques available. Two methods that are both sensitive and very fast are Secondary Emission Monitors (SEMs) [21] and Faraday cups [22]. Since the time resolution of these devices is determined by the geometry required to collect the signal, they can be almost arbitrarily fast, and simple examples have been constructed with resolutions of 150 ps, as shown in Figure 21.

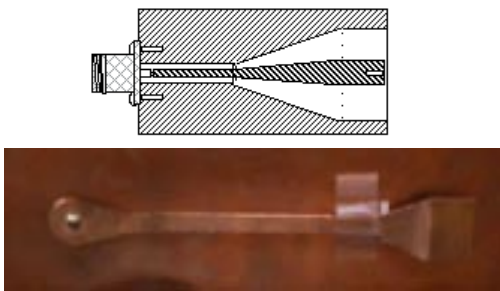


FIG. 21. (Coaxial) Faraday and (stripline) SEM prototypes.

Measurements of prototype systems are underway at the Bldg 211 linac at Argonne. Preliminary measurements on impedance matched pickups of various geometries have shown that it is comparatively simple to produce time resolutions limited by the dimensions of the pickup elements themselves. The signals produced, $V = I_{beam}R$, are in the range of 30 kV (which are seen in tests) for primary accelerator beams, though smaller for secondary beams. Sampling scopes have been used for recording the signals.

The minimum useful signal from an electronic detector is constrained by thermal noise. This can be expressed as

$$V_{noise} = \sqrt{4P_{noise}/R} = \sqrt{4 \Delta f kT NF R/N_p},$$

where P_{noise} is the noise power, and Δf , kT , NF , R , N_p are the bandwidth of the system, the thermal energy, the preamp noise figure, the input resistance and the number of traces that can be averaged to give a final result [23] [24] [25].

In addition to the rf induced backgrounds, there will be both backgrounds due to other particles in the beam and due to muon halos in six dimensions. Most of backgrounds due to other particles can be isolated by means of particle range and timing. Muon halos will require careful simulation, measurements and then subtraction. These measurements will require instrumentation with comparatively large dynamic range, which again is available with SEMs and Faraday cups. These two techniques could also be used very effectively in a real machine.

D. Other Instrumentation

The cooling experiment might usefully employ a final spectrometer at the end of the cooling section which would be able to produce independent measurements of the six dimensional bunch distribution to correlate with the longitudinal bunch measurements. While a bent solenoid would be useful in this application, it might be somewhat cheaper to use a more conventional iron dipole, if the optical match between the solenoidal optics and the conventional optics can be done easily.

Some other constraints are relevant. One of the more simple is that the range of low energy muons in solids is very short. The range momentum curves for muons and electrons is shown in Figure 22. This short range makes collimators work quite well, since the multiple scattering angles are quite large. Comparable electron ranges require beam energies of about 20 MeV, thus many low energy electron accelerators are useful for diagnostic development.

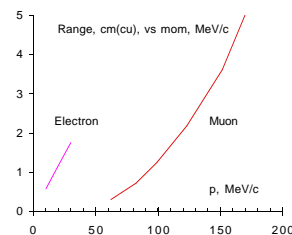


FIG. 22. the ranges of electrons and muons in copper.

The secondary emission coefficients used in CERN beam SEMs have been shown to depend on the total

beam flux hitting the detector. This has been documented in a note [26].

Scintillators have many advantages, and will probably be used in many applications, however scintillation processes depend on atomic recombination rates and these tend to be somewhat slow. The damping rate for an atomic oscillator has been derived many places (Panofsky and Phillips for example [27]) and is neatly parameterized for all materials by Siegman [28] as,

$$\tau_{rad}[ns] = \frac{45\lambda^2}{n},$$

where λ and n are the wavelength of the emitted photon, in microns, and the refractive index of the material. In commercial scintillators, the rates have been speeded up with the addition of other compounds with vibrational levels nearby. Liquid hydrogen may be too cold to allow significant amounts of helpful additives [29].

VI. FACILITIES

This experiment could be performed at a number of locations. The TT1 transfer line between the CERN PS and ISR building may be very good location and the figure gives the approximate size of the decay line and cooling equipment. The tunnel is about 4 m wide, 140 m long, and straight, and it seems to have good access at the downstream end [30].

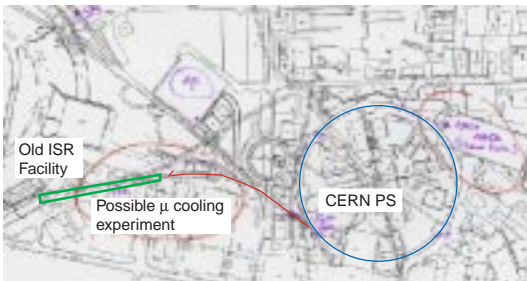


FIG. 23. The CERN option.

At Fermilab, the MI-40 beam dump would be useful as would any line in the meson building although these are not presently operational. The AGS has fast extracted beams, but the bunch length may be difficult to reduce below the 2 ns already achieved without a higher frequency rf system in the ring although the cost of this system might be small in comparison with the rest of the experiment.

VII. PROBLEMS

There are a number of open issues, many are quite independent problems. Some are controversial. The start

of a list: What are the optimum experimental parameters? How low can the momentum be? How high can the rf frequency be? Are there other ways of making the cooling system more efficient? How important is it to use the parameters of the final machine? What is the optimum beam line? (solenoid, Quad, . . .) How short a proton bunch can be produced? What are the backgrounds? How many 440 MeV/c pions are transmitted by 80 cm of Be? Simulation and optimization of the beamline. What measurements and instrumentation are required?

-
- [1] R. Fernow, ICOOL: a Simulation Code for Ionization Cooling of Muon Beams, Proceedings of the 1999 Particle Accelerator Conference, New York (1999) 3020
 - [2] J. Monroe, P. Lebrun, P. Spentzouris, DPGent and ICOOL Code Comparison, MUCOOL Note no. 72
 - [3] Kwang-Je Kim and Chun-xi Wang, Phys. Rev. Lett., 85 (00) 760
 - [4] G. Penn and J. S. Wurtele, Phys. Rev. Lett., 85, (00), 764
 - [5] V. Balbekov, P. Lebrun, J. Monroe, P. Spentzouris, MUCOOL Note 125 (2000)
 - [6] A Feasibility Study of a Neutrino Source Based on a Muon Storage Ring http://www.fnal.gov/projects/muon_collider/nufactory/fermi_study_after_april1st/
 - [7] Palmer SFOFO, at http://pubweb.bnl.gov/people/gallardo/mutac_2000/palmer2.ps
 - [8] Caso et al. Eur. Phys. J Jour. C3 (98) 1
 - [9] K. McDonald, "Comments on Ionization Cooling" MuMu/98/17 at <http://www.hep.princeton.edu/mumu>.
 - [10] J. Norem Mucool Note #21, 1999
 - [11] V. Balbekov, St Croix Group Meeting, May 1999
 - [12] V. Balbekov Fermilab Private Communication (2000)
 - [13] David Neuffer, $e^+ + e^-$ Colliders, CERN Yellow Report 99-12.
 - [14] C. Ankenbrandt et al, Phys. Rev. Spec. Top. -Accel. and beams 1 (98) 030101
 - [15] D Carey
 - [16] D. Marisseau, New England TechniCoil, (2000)
 - [17] D. Spooner, Dexter Magnetic Technologies, (2000)
 - [18] N. Mokhov, Fermilab, Private Communication, 2000
 - [19] J. Norem, A. Moretti, and M. Popovic, MUCOOL Note 139, 2000
 - [20] R. Silbergliitt, FM Technologies, Inc., Fairfax VA, Private communication 2000
 - [21] J. Borer and R. Jung, Diagnostics, in CERN Accelerator School, Anti protons for Colliding Beam Facilities, CERN yellow report 84-15, 1984
 - [22] G. Beck and D. W. Schutt, Rev. of Sci. Instrum. 43 (1972) 341
 - [23] J. B. Johnson, Phys. Rev., 32 (28), 97
 - [24] H. Nyquist, Phys. Rev., 32 (28), 110
 - [25] L. Chetuck, Miteq Corp, Private Communication (2000)

- [26] G. Ferioli and R. Jung, CERN Report CERN-SL 97-71(BI), (1997)
- [27] W. K. H. Panofsky, and M. Phillips, Classical Electricity and Magnetism, Second Ed, Addison-Wesley, Reading Mass, 1962, Chapter 22.
- [28] A. Siegman, Lasers, University Science Books, Mill Valley CA, 1986, p121
- [29] C. Jonah, ANL/CHM, Private Communication 2000
- [30] R. Cappi, at <http://alephwww.cern.ch/~bd/muon/mini/agenda.html>